










RESEARCH ARTICLE

Analytical profile, in vitro metabolism and behavioral properties of the lysergamide 1P-AL-LAD

Simon D. Brandt¹  | Pierce V. Kavanagh²  | Folker Westphal³  |
Benedikt Pulver^{3,4,5}  | Hannes M. Schwelm^{4,5}  | Kyla Whitelock⁶  |
Alexander Stratford⁷  | Volker Auwärter⁴  | Adam L. Halberstadt^{6,8} 

¹School of Pharmacy and Biomolecular Sciences, Liverpool John Moores University, Liverpool

²Department of Pharmacology and Therapeutics, School of Medicine, Trinity Centre for Health Sciences, St. James Hospital, Dublin 8, Ireland

³State Bureau of Criminal Investigation Schleswig-Holstein, Section Narcotics/ Toxicology, Kiel, Germany

⁴Institute of Forensic Medicine, Forensic Toxicology, Medical Center, Faculty of Medicine, University of Freiburg, Freiburg, Germany

⁵Hermann Staudinger Graduate School, University of Freiburg, Freiburg, Germany

⁶Department of Psychiatry, University of California San Diego, La Jolla, California, USA

⁷Synex Synthetics BV, Maastricht, The Netherlands

⁸Research Service, VA San Diego Healthcare System, San Diego, California, USA

Correspondence

Simon D. Brandt, School of Pharmacy and Biomolecular Sciences, Liverpool John Moores University, Byrom Street, Liverpool L3 3AF, UK.

Email: s.brandt@ljmu.ac.uk

Funding information

Internal Security Fund of the European Union, Grant/Award Number: IZ25-5793-2019-33; National Institute on Drug Abuse (NIDA), Grant/Award Number: R01 DA041336

Abstract

Lysergic acid diethylamide (LSD) is known to induce powerful psychoactive effects in humans, which cemented its status as an important tool for clinical research. A range of analogues and derivatives has been investigated over the years, including those classified as new psychoactive substances. This study presents the characterization of the novel lysergamide *N,N*-diethyl-1-propanoyl-6-(prop-2-en-1-yl)-9,10-didehydroergoline-8 β -carboxamide (1P-AL-LAD) using various mass spectrometric, gas- and liquid chromatographic and spectroscopic methods. In vitro metabolism studies using pooled human liver microsomes (pHLM) confirmed that 1P-AL-LAD converted to AL-LAD as the most abundant metabolite consistent with the hypothesis that 1P-AL-LAD may act as a prodrug. Fourteen metabolites were detected in total; metabolic reactions included hydroxylation of the core lysergamide ring structure or the *N*⁶-allyl group, formation of dihydrodiol metabolites, *N*-dealkylation, *N*¹-deacylation, dehydrogenation, and combinations thereof. The in vivo behavioral activity of 1P-AL-LAD was evaluated using the mouse head twitch response (HTR), a 5-HT_{2A}-mediated head movement that serves as a behavioral proxy in rodents for human hallucinogenic effects. 1P-AL-LAD induced a dose-dependent increase in HTR counts with an inverted U-shaped dose-response function, similar to lysergic acid diethylamide (LSD), psilocybin, and other psychedelics. Following intraperitoneal injection, the median effective dose (ED₅₀) for 1P-AL-LAD was 491 nmol/kg, making it almost three times less potent than AL-LAD (174.9 nmol/kg). Previous studies have shown that *N*¹-substitution disrupts the ability of lysergamides to activate the 5-HT_{2A} receptor; based on the in vitro metabolism data, 1P-AL-LAD may induce the HTR because it acts as a prodrug and is metabolized to AL-LAD after administration to mice.

KEYWORDS

5-HT_{2A} receptor, LSD, new psychoactive substances, psychedelics

This is an open access article under the terms of the [Creative Commons Attribution-NonCommercial](https://creativecommons.org/licenses/by-nc/4.0/) License, which permits use, distribution and reproduction in any medium, provided the original work is properly cited and is not used for commercial purposes.

© 2022 The Authors. *Drug Testing and Analysis* published by John Wiley & Sons Ltd.

1 | INTRODUCTION

The classical psychedelic lysergic acid diethylamide (LSD, Figure 1) has long been known for its ability to induce complex, non-ordinary states of consciousness in humans.^{1–3} Over the last decade, psychedelic drugs such as LSD and psilocybin have been explored as potential treatments for a variety of psychiatric disorders, including anxiety, treatment-resistant depression, anorexia, drug and alcohol dependence, cluster headaches, and obsessive–compulsive disorder.^{4–8} At the same time, recreational use of LSD and other psychedelic drugs continues to occur though the prevalence of use varies widely across countries and age groups.^{9,10}

Extensive modifications of the LSD structural scaffold have been investigated. Studies characterizing the structure–activity relationships for LSD have frequently focused on the amide substituents although some exceptions exist. The majority of changes made to the *N,N*-diethyl group were found to reduce potency.^{11,12} Another structural modification that has been explored is the replacement of the LSD *N*⁶-methyl group with other substituents. For example, Niwaguchi and co-workers reported the synthesis of *N*⁶-ethyl-nor-LSD (ETH-LAD), *N*⁶-*n*-propyl-nor-LSD (PRO-LAD), and *N*⁶-allyl-nor-LSD (AL-LAD) (Figure 1 for ETH-LAD and AL-LAD) in 1976.¹³ All three lysergamides showed greater oxytocic activity than LSD in rat uterine tissues.¹⁴ Likewise, AL-LAD was also shown to induce a stronger hyperthermic response than LSD in rabbits.¹⁵ In 1985, Hoffman and Nichols published on the behavioral evaluation of ETH-LAD, PRO-LAD, AL-LAD, as well as three other *N*⁶-substituted lysergamides and tested them in a drug discrimination assay in which rats were trained to discriminate 0.08 mg/kg LSD from saline. The LSD derivatives containing *N*⁶-ethyl (ETH-LAD), *N*⁶-*n*-propyl (PRO-LAD), *N*⁶-allyl (AL-LAD), *N*⁶-isopropyl (IPR-LAD), and *N*⁶-*n*-butyl (BU-LAD) substituents produced full substitution in LSD-trained rats.

Notably, while PRO-LAD had about the same potency as LSD, ETH-LAD and AL-LAD were more potent than LSD in the drug discrimination paradigm.¹⁶

Anecdotal reports suggest that oral administrations of ETH-LAD, PRO-LAD, and AL-LAD produce psychedelic-like effects in humans.¹⁷ Consistent with the rat drug discrimination data, ETH-LAD was slightly more potent than LSD in humans whereas AL-LAD was approximately equipotent.^{17,18} In recent years, both AL-LAD and ETH-LAD became available for purchase from online retailers, often distributed on small pieces of absorbent paper (“blotters”).^{19,20} Reports describing their detection were first notified to the European Monitoring Centre for Drugs and Drug Addiction (EMCDDA) in 2015 and 2016, respectively.^{21,22} Since then, other publications have appeared describing the detection of AL-LAD and ETH-LAD by researchers located outside of Europe.^{23,24}

Investigations carried out *in vitro* where ETH-LAD and AL-LAD were incubated with pooled human liver S9 microsomal fraction detected five ETH-LAD metabolites and 11 AL-LAD metabolites. Furthermore, studies using selective inhibitors of cytochrome P450 (CYP) enzymes showed that CYP3A4 was involved in *N*⁶-dealkylation and *N*-deethylation reactions (ETH-LAD and AL-LAD), whereas CYP2D6 and CYP3A4 (ETH-LAD) and CYP1A2 and CYP3A4 (AL-LAD) were responsible for various hydroxylations; phase 2 glucuronide metabolites were also detected.²⁵

In addition to the *N,N*-diethylamide group of LSD and the *N*⁶-position, various substitutions have been made to the indole nitrogen (position *N*¹). Among the earliest examples were 1-methyl-LSD (MLD-41) and 1-acetyl-LSD (ALD-52). More recently, a number of novel 1-acyl-substituted lysergamides have emerged on the market (Figure 1). 1-Propanoyl-LSD (1P-LSD) first appeared in 2016, followed by 1-butanoyl-LSD (1B-LSD), 1-valeroyl-LSD (1V-LSD), and 1-cyclopropanoyl-LSD (1cP-LSD).^{20,26–29} One complexity with these

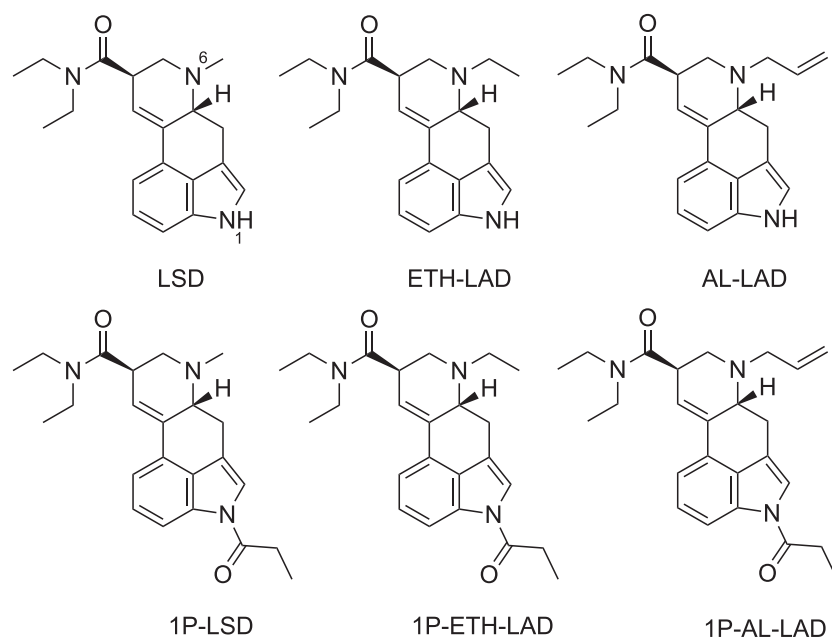


FIGURE 1 Chemical structures of lysergic acid diethylamide (LSD) and *N*⁶-modified analogs and their *N*¹-propanoyl derivatives

molecules is that substitution on the indole nitrogen reduces the affinity of ergolines for the 5-HT_{2A} receptor,^{30,31} the site responsible for mediating the characteristic effects of psychedelic drugs. However, the 1-acyl group appears to be rapidly hydrolyzed in vivo, so the activity of these lysergamides is likely dependent on their metabolism to LSD.

In addition to LSD, the 1-acyl derivatives of other lysergamides have also been synthesized. 1-Propanoyl-ETH-LAD (1P-ETH-LAD), the first known example, appeared online in 2016 and its detection was first notified to the EMCDDA in 2017.³²

The present investigation continues the research on novel lysergamides and reports on the analytical properties of *N,N*-diethyl-1-propanoyl-6-(prop-2-en-1-yl)-9,10-didehydroergoline-8 β -carboxamide (1-propanoyl-AL-LAD; 1P-AL-LAD), the *N*¹-propanoyl derivative of the psychedelic drug 6-allyl-norlysergic acid diethylamide (AL-LAD) (Figure 1). There is no indication that this compound is currently available for sale by Internet retailers but it was considered prudent that its analytical profile should be made available to stakeholders involved in psychoactive drug research. Because 1P-AL-LAD is expected to act as a prodrug for AL-LAD, experiments were conducted to determine whether 1P-AL-LAD is *N*¹-deacylated in vitro after incubation with pooled human liver microsomes (pHLM). Finally, 1P-AL-LAD was evaluated in the mouse head-twitch response (HTR) assay to test whether it has an LSD-like behavioral profile.^{33–35}

2 | EXPERIMENTAL

2.1 | Materials

Formic acid (Rotipuran[®] \geq 98%, p.a.) and potassium hydrogen phosphate (\geq 99%, p.a.) were obtained from Carl Roth (Karlsruhe, Germany); acetonitrile (ACN) (LC–MS grade), aqueous ammonium formate solution (10 M, \geq 99.995% trace metals basis), and potassium hydroxide [puriss. p.a. \geq 86% (T) pellets] from Sigma-Aldrich (Steinheim, Germany); pHLM (150 donors, 20 mg/ml protein in 250 mM sucrose), nicotinamide adenine dinucleotide phosphate (NADPH) regenerating solutions A and B (reductase activity 0.43 μ mol/min/ml), and potassium phosphate buffer 0.5 M (pH 7.5) from Corning (Corning, NY, USA). Other chemicals and solvents were of analytical and HPLC grade and obtained from Aldrich (Dorset, UK). 1P-AL-LAD hemitartrate (2:1) ($>$ 95%) powder was supplied by Synex Synthetics BV, Maastricht, The Netherlands.

2.2 | Instrumentation

2.2.1 | Gas chromatography-electron ionization-mass spectrometry (GC-EI-MS)

Approximately 1 mg of the sample was dissolved in 10 ml of methanol and diluted 1:10. A Finnigan TSQ 8000 triple stage quadrupole mass spectrometer coupled to a Trace GC Ultra gas chromatograph

(Thermo Fisher, Waltham, USA) and equipped with a fused silica DB-1 column (30 m x 0.32 mm i.d., 0.25 μ m film thickness) (Agilent Technologies, Santa Clara, USA) was used for GC-EI-MS analysis. Sample solutions were introduced by a CTC CombiPAL (CTC Analytics, Zwingen, Switzerland) autosampler.

The following GC parameters were employed: injection volume: 0.5 μ l, splitless; injector temperature: 280°C; carrier gas: helium; flow rate: 1.2 ml/min. Initially, the oven temperature was kept at 80°C for 2 min, ramped to 310°C at 20°C/min and subsequently maintained at the final temperature of 310°C for 23 min. MS parameters were set as follows: ionization mode: EI at 70 eV; emission current: 50 μ A; ion source temperature: 220°C; MS transfer line temperature: 300°C; scan time: 1 s; scan range: *m/z* 29–600.

Data analysis was conducted using Xcalibur 4.0 Qual Browser (Thermo Fisher) and the National Institute of Standards and Technology (NIST) MS search program (version 2.3) (NIST, MD, US). EI mass spectra were compared with EI mass spectral libraries provided by the NIST (release 2020), the European Network of Forensic Science Institutes (ENFSI, release 2018), Scientific Working Group for the Analysis of Seized Drugs (SWGDRUG, release 2021), as well as the designer drug library 2021 (DigiLab, SH, DE) and libraries built in-house. Retention indices (RI) were calculated from the measurement of retention times obtained from the constituents of an *n*-alkane mixture. The temperature program is specified above. For calculation, logarithmic interpolation was applied between two consecutive *n*-alkanes.

2.2.2 | Gas chromatography-solid-phase-infrared analysis (GC-sIR)

A GC-solid phase-IR-system consisting of an Agilent GC 7890B (Agilent Technologies) equipped with a fused silica capillary DB-1 column (30 m x 0.32 mm internal diameter, 0.25 μ m film thickness), an Agilent G4567A probe sampler (Agilent Technologies) and a DiscovIR-GC (Spectra Analysis, Marlborough, MA, US) were used for the acquisition of solid transmission IR spectra. The eluting substances were cryogenically accumulated on a spirally rotating ZnSe disk cooled by liquid nitrogen to -40°C . IR spectra were recorded through the IR-transparent ZnSe disk using a nitrogen-cooled mercury cadmium telluride (MCT) detector.

The GC parameters were as follows: injection volume 1 μ l; splitless mode; injection port temperature 240°C; carrier gas: helium; flow rate 2.5 ml/min. Chromatographic conditions were as follows: oven temperature program: 80°C for 2 min, ramped to 310°C at 20°C/min, and maintained for 20 min; transfer line: 280°C. Infrared conditions: oven temperature 300°C; restrictor temperature 300°C; disc temperature -40°C ; dewar cap temperature 35°C; vacuum 0.2 mTorr; disc speed 3 mm/min; spiral separation 1 mm; wavelength resolution 4 cm^{-1} ; IR range 650–4000 cm^{-1} ; acquisition time: 0.6 s/file and 64 scans per spectrum. Data were processed using GRAMS/AI Ver. 9.1 (Grams Spectroscopy Software Suite, Thermo Fisher) followed by OMNIC Software, Ver. 7.4.127 (Thermo Fisher).

2.2.3 | High performance liquid chromatography electrospray ionization quadrupole time-of-flight mass spectrometry (HPLC-ESI-QTOF-MS) experiments

HPLC-ESI-QTOF-MS analysis was performed on an impact II™ QTOF instrument coupled with an Elute HPLC system (both from Bruker Daltonik, Bremen, Germany). Chromatographic separation was achieved on a Kinetex® Biphenyl column (100 × 2.1 mm, 2.6 μm particle size, Phenomenex, Aschaffenburg, Germany) equipped with a corresponding guard column (SecurityGuard™ ULTRA Cartridges UHPLC Biphenyl for columns with an internal diameter of 2.1 mm, Phenomenex, Aschaffenburg, Germany). HPLC mobile phase A consisted of deionized water (979 ml), formic acid (1 ml), ammonia formate (200 mM, 10 ml, freshly prepared from aqueous 10 M solution) and ACN (10 ml). Mobile phase B consisted of acetonitrile (989 ml), formic acid (1 ml) and ammonia formate (200 mM, 10 ml, freshly prepared from aqueous 10 M solution). Mobile phase A and B were varied in a linear program ($T_{\text{min}}/A:B$; $T_0/90:10$; $T_{10}/20:80$; $T_{10.5-12.5}/5:95$; $T_{12.7-14}/90:10$) with LC flow set at 0.3 ml/min and column oven temperature at 40°C. The autosampler was cooled to 5°C. The injection volume was 10 μl. HyStar™ version 3.2 and DataAnalysis version 4.2 (both from Bruker Daltonik) were used for data acquisition and processing, respectively. The QTOF-MS was operated in positive electrospray ionization mode acquiring spectra in the range of m/z 50–500 (acquisition rate of 4.0 Hz). Acquisition was performed in full scan/broadband collision induced dissociation (bbCID) mode (data independent) and in a second run in full scan/AutoMS/MS mode (data dependent) to obtain cleaner fragment spectra. The collision energy applied for bbCID and Auto-MS/MS was 30 ± 6 eV. The dry gas temperature was set to 200°C with a dry gas flow of 8.0 L/min. The nebulizer gas pressure was 200 kPa. Nitrogen was used as collision gas. The voltages for the capillary and end plate offset were 2500 and 500 V, respectively. External and internal mass calibrations were performed using sodium formate/acetate clusters and high precision calibration (HPC) mode. Metabolites generated in the pHLM assay were tentatively identified and characterized in manual data processing with the following criteria: mass error of the precursor ion < 5 ppm, signal-to-noise ratio > 3:1, and mass tolerance for fragment ions ± 10 ppm.

2.2.4 | Pooled human liver microsome (pHLM) assay

Total assay volume of 100 μl consisted of 5 μl pHLM solution, 1 μl 1P-AL-LAD stock solution (1 mg/ml in ACN), 5 μl NADPH regenerating solution A, 1 μl NADPH regenerating solution B, 20 μl phosphate buffer, and 58 μl deionized water. Incubation was conducted for 30 min at 37°C. The incubation was quenched by adding 300 μl of ice-cold acetonitrile. Ammonium formate (50 μl, 10 M) was added for improved phase separation and after centrifugation the organic layer was transferred into a separate vial and stored at –20°C. Incubations were performed in triplicate. Additionally, two negative control

samples were processed in the same way. One was performed with 5 μl phosphate buffer instead of pHLM to identify compounds not formed by metabolism, and a second with 1 μl ACN instead of the substrate to confirm the absence of interfering compounds. For LC-ESI-QTOF-MS analysis, 100 μl supernatant was evaporated dryness under a gentle stream of nitrogen and reconstituted in 50 μl mobile phase A/B (70:30, v/v).

2.3 | Animal pharmacology

Male C57BL/6J mice (6–8 weeks old) from Jackson Labs (Bar Harbor, ME, USA) were used for the behavioral experiments. The mice were housed on a reversed light–dark cycle (lights on at 1900 h, off at 0700 h,) in a vivarium approved by the Association for Assessment and Accreditation of Laboratory Animal Care (AAALAC) at the University of California San Diego. Mice were housed up to four per cage in a climate-controlled room and with food and water provided ad libitum except during behavioral testing. Testing was performed between 1000 and 1800 h (during the dark phase of the light–dark cycle). The studies were conducted in accordance with National Institutes Health (NIH) guidelines and were approved by the University of California San Diego Institutional Animal Care and Use Committee. 1P-AL-LAD hemitartrate (2:1) was dissolved in isotonic saline for intraperitoneal (IP) injection (5 ml/kg).

The head-twitch response (HTR) was assessed using a head-mounted neodymium magnet and a magnetometer detection coil. The magnet was attached as described previously³⁴ and then the mice were allowed to recover from the surgeries for at least 1 week prior to behavioral testing. HTR experiments were conducted in a well-lit room, and the mice were allowed to habituate to the room for at least 1 h prior to testing. Mice ($n = 5\text{--}6/\text{group}$, 32 total) were injected IP with vehicle or 1P-AL-LAD and then placed in a 12-cm diameter glass cylinder surrounded by a magnetometer coil; activity was recorded continuously for 30 minutes. Coil voltage was low-pass filtered (1 kHz), amplified, and digitized (20-kHz sampling rate) using a Powerlab/8SP with LabChart v 7.3.2 (ADInstruments, Colorado Springs, CO, USA). Head twitches were identified in the recordings using artificial intelligence.³⁶ HTR counts were analyzed using a one-way Welch ANOVA. Dunnett's T3 multiple comparisons test was used for post hoc comparisons. Significance was demonstrated by surpassing an alpha level of 0.05. Median effective doses (ED₅₀ values) and 95% confidence intervals for dose–response experiments were calculated by nonlinear regression (Prism 9.01, GraphPad Software, San Diego, CA, USA).

3 | RESULTS AND DISCUSSION

3.1 | Analytical features

The electron ionization (EI) mass spectrum of 1P-AL-LAD is shown in Figure 2a with suggested fragmentation pathways included in the

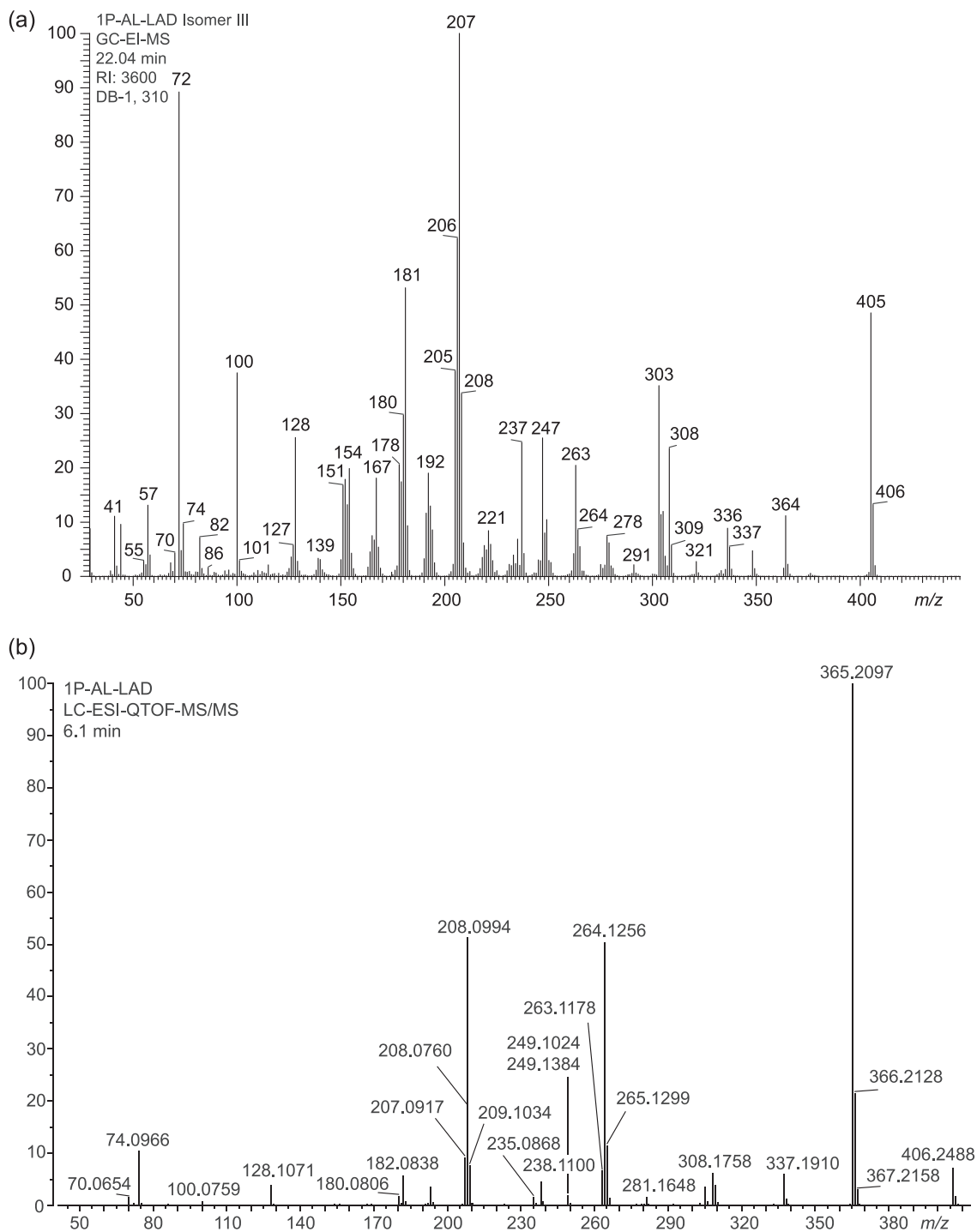


FIGURE 2 (a) Electron ionization mass spectrum of 1P-AL-LAD (isomer III). (b) Electrospray ionization QTOF tandem mass spectrum of 1P-AL-LAD

supporting information. In comparison with AL-LAD reported previously,¹⁹ and other LSD-related compounds, a group of key ions were detectable in the form of fragment clusters including m/z 151–156, m/z 161–169, m/z 178–182, m/z 191–197, and m/z 205–208. Similar to other lysergamides with a N,N -diethylamide group, iminium ions were detected at m/z 72 together with m/z 100 and m/z 128.^{19,20,26–29} Compared with AL-LAD, the presence of the propanoyl

group shifted some of the ions by 56 Da including the molecular ion at m/z 405 (AL-LAD: m/z 349), the *retro*-Diels-Alder fragment following the loss of N -allylmethanimine at m/z 336 (AL-LAD: m/z 280), or the species reflecting the loss of the N^6 -allyl group at m/z 364 (AL-LAD: m/z 308).¹⁹ A characteristic oxonium ion reflecting the presence of the N^1 -propanoyl substituent was also observed at m/z 57, which was comparable to other N^1 -propanoyl lysergamides such

as 1P-LSD²⁶ and 1P-ETH-LAD.²⁰ An extracted ion chromatogram (EIC; m/z 405) obtained from the GC-MS analysis of a methanolic solution of 1P-AL-LAD is shown in the supporting information to consider the detection of 1P-AL-LAD isomers including iso-1P-AL-LAD. Three minor isomers were detected under the conditions used with 1P-AL-LAD being labeled as isomer III. The EI mass spectral data for isomers I, II, and IV are shown in the supporting information. The epimeric iso-1P-AL-LAD was expected to show a comparable electron ionization mass spectrum but it appeared that the recorded spectra showed distinct differences (for example the presence of m/z 333 at high abundance especially for isomers I and II), which led to the tentative suggestion that the detected isomers might not have reflected the detection of iso-1P-AL-LAD but rather GC-induced by-products (not detectable under LC-MS conditions, see below). However, these suggested structures were based on mass spectral grounds alone and in the absence of suitable reference material these proposals must remain speculative. As shown below, however, analysis of 1P-AL-LAD by LC-MS suggested the detection of iso-1P-AL-LAD at low abundance.

A full scan GC-MS trace of this analysis has also been provided as supporting information and further inspections revealed another peak eluting at 23.08 min, labeled as 1P-AL-LAD-A ($-C_3H_8$). The molecular ion was detected at m/z 361 and together with the information shown in the mass spectrum, it was thought that this compound may have represented the N^6 -dealkylated, fully aromatic (D-ring) derivative (supporting information). Similar to the minor isomers, it was hypothesized that the formation of 1P-AL-LAD-A ($-C_3H_8$) was also GC-induced. Finally, the TIC trace also showed a peak at 18.00 min, which was identified as AL-LAD consistent with the information obtained from LC-MS analysis described below. Interestingly, LSD formation during GC-MS analysis of 1P-LSD has been described by Tanaka and colleagues,²³ which suggests that the potential for such artificial formations might need to be considered in cases where the N^1 -acylated form is not a controlled substance. In the laboratories of the authors, however, this artificial formation has not yet been observed. Basification followed by extraction into diethyl ether led to hydrolysis to AL-LAD when subjected to GC-MS analysis. The three minor isomers and 1P-AL-LAD-A ($-C_3H_8$) were also detected (full scan, supporting information).

The ESI-QTOF tandem mass spectrum recorded for 1P-AL-LAD after incubation with pHLM is shown in Figure 2b (proposed fragmentation pathways in the supporting information). The base peak was detected at m/z 365.2097 consistent with a homolytic loss of the N^6 -allyl group and formation of a radical cation ($C_{22}H_{27}N_3O_2^{*\cdot+}$), similar to a previous report with AL-LAD where this loss also occurred to a significant extent.¹⁹ For ETH-LAD and 1P-ETH-LAD, the corresponding loss of the N^6 -ethyl group was observed as well although the resulting ions did not reach base peak abundance.²⁰ A neutral loss of N,N -diethylformamide from the m/z 365.2097 ion might have led to a further dissociation to $C_{17}H_{18}N_2O^{*+}$ (m/z 264.1256) followed by detection of $C_{14}H_{12}N_2^{*+}$ (m/z 208.0994), reflecting the subsequent cleavage of the N^1 -acyl group. The species at m/z 337.1910 ($C_{21}H_{25}N_2O_2^+$) might have reflected the

involvement of a *retro*-Diels-Alder mechanism (neutral loss of N -allylmethanimine) and was also thought to be the same ion formed in the spectra of 1P-LSD²⁶ and 1P-ETH-LAD.²⁰ The mass spectral resolution was also sufficient to detect another m/z 208 species (m/z 208.0760, $C_{14}H_{10}NO^+$) possibly representing an oxonium species following an alternative pathway (supporting information), which then might have resulted in the formation of m/z 180.0806 ($C_{13}H_{10}NO^+$). Two m/z 249 ions were also observed with minor abundance (Figure 2b). One of them was detected at m/z 249.1384 ($C_{17}H_{17}N_2^+$) that might have resulted from 1P-AL-LAD following a consecutive loss of the propanoyl group and N,N -diethylformamide. The other ion was observed at m/z 249.1024 ($C_{17}H_{17}N_2^+$) that could have arisen from the m/z 264.1256 radical cation after losing a methyl radical. Fragment ions that might have formed from the carboxamide moiety included m/z 128.1071 ($C_7H_{14}NO^+$), 100.0759 ($C_9H_{10}NO^+$), and 74.0966 ($C_4H_{12}N^+$). The presence of the N^6 -allyl substituent might have been reflected by the ion at m/z 70.0654 (protonated N -allylmethanimine, $C_4H_8N^+$). Additional QTOF tandem mass spectra recorded from 1P-AL-LAD on a different instrument (Agilent 6530B) can also be found in the supporting information. In addition, multi-stage MSⁿ data recorded from a direct infusion using a linear ion trap (LIT) mass spectrometer have also been added in the supporting information.

The GC-MS results described above suggested that iso-1P-AL-LAD remained undetectable based on mass spectral considerations. The implementation of LC-ESI-QTOF-MS analysis however indicated that the epimer was detectable both in a 1P-AL-LAD solution and in a negative pHLM mixture. Based on a comparison of signal responses involving peak heights, the percentage value for the iso-form was estimated to be around 1.12% (supporting information). As described above, the GC-MS analysis also revealed the detection of AL-LAD (supporting information), which raised the question as to whether it was potentially GC-induced or present as an impurity, or both. LC-ESI-QTOF-MS analysis confirmed that AL-LAD could be detected as an impurity in the 1P-AL-LAD sample estimated to represent around 0.64%, which was considered low. This estimation was based on a comparison with the signal response recorded for AL-LAD at a $1 \mu\text{g/ml}$ concentration (supporting information). For the purpose of the *in vitro* metabolism study described below, analysis of the incubation mixture without addition of pHLM also confirmed the detection of iso-1P-AL-LAD and AL-LAD. In the latter case, however, it could not be established whether some proportion of the detected peak was also formed after non-enzymatic hydrolysis (supporting information). An alternative LC-ESI-linear ion trap-MS/MS method was also employed and it could be confirmed that AL-LAD was detectable in the 1P-AL-LAD sample as well (supporting information).

When analyzing solutions of 1P-AL-LAD and negative pHLM, the EIC at m/z 422.2434 ($C_{25}H_{32}N_3O_3^+$) revealed the detection of additional peaks (supporting information). Though the signal intensity seemed low ($\sim 0.28\%$), the QTOF-MS/MS data of the peak at 6.9 min suggested the presence of a hydroxylated 1P-AL-LAD species and further inspection of the mass spectral data suggested that the hydroxylation might have occurred on the 7-position (Figure 3). The majority

of product ions appeared to be comparable to those detected with 1P-AL-LAD (Figure 2) but some noticeable differences were also observed. The detection of the *retro*-Diels Alder fragment (m/z 337.1909 (similar to 1P-AL-LAD, Figure 2b and supporting information) initially suggested that the hydroxylation must have occurred on the part of the molecule that would have been lost during the formation of m/z 337.1909 ($C_{21}H_{25}N_2O_2^+$). An important key indicator for the tentative identification of 7-HO-1P-AL-LAD arose from the

detection of m/z 381.2047 ($C_{22}H_{27}N_3O_3^{*+}$) representing the loss of the N^6 -allyl radical, which in turn suggested that the hydroxylation could not have occurred on the allyl group. As shown in Figure 2b, the radical loss of the N^6 -allyl group attached to 1P-AL-LAD was seen at m/z 365.2097 ($C_{22}H_{27}N_3O_2^{*+}$) whereas in the hydroxylated impurity, this was not detected. Instead, a mass shift consistent with an additional hydroxyl group gave rise to m/z 381.2047 albeit at low abundance. The presence of the hydroxyl group that supported the

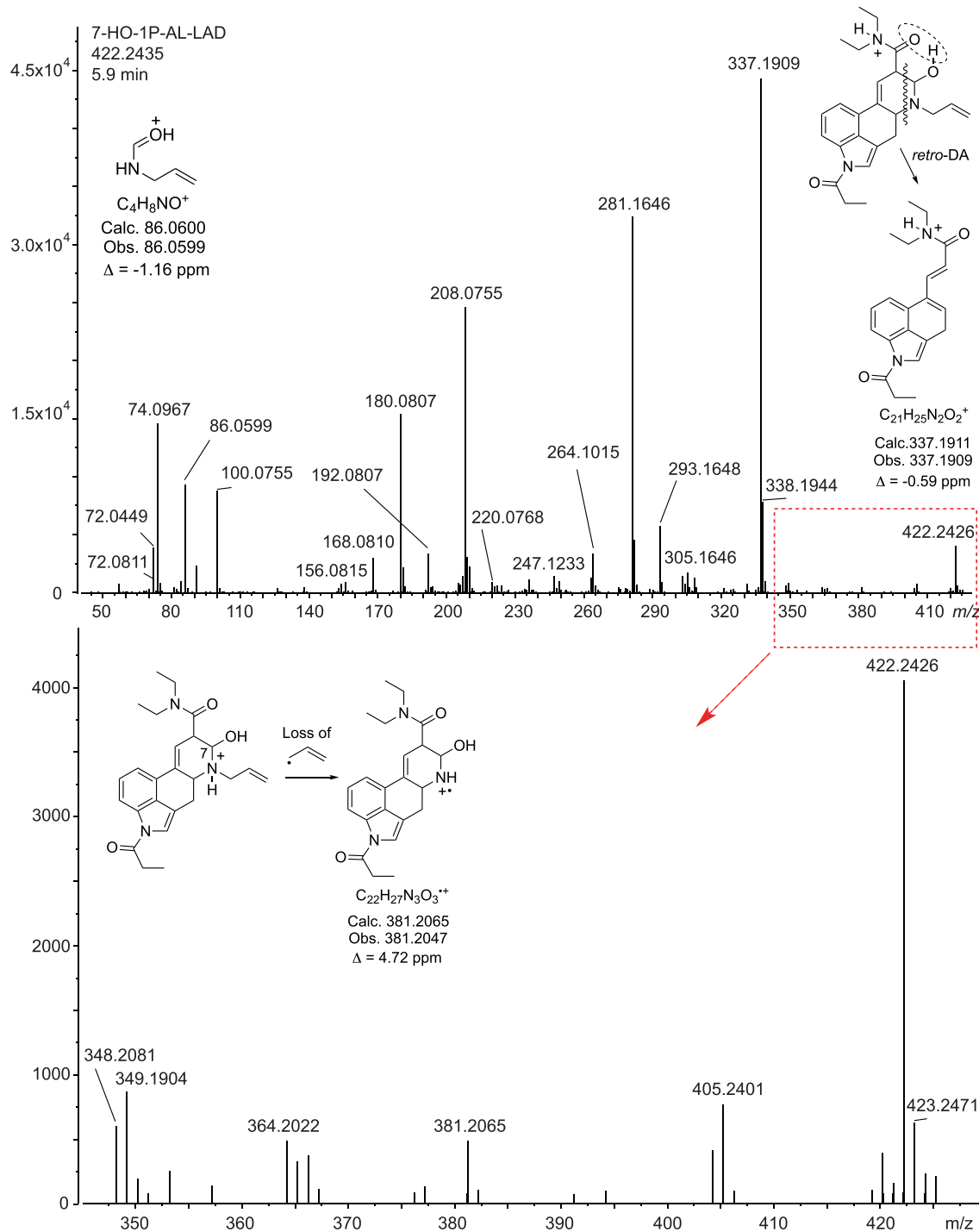
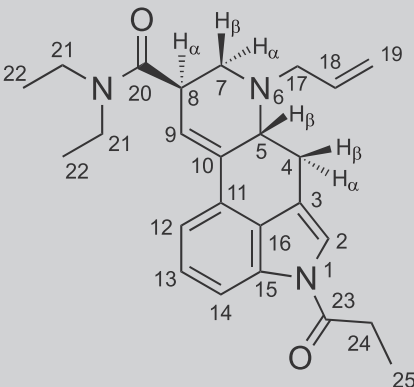
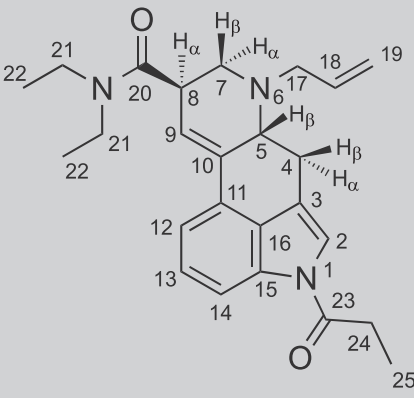


FIGURE 3 Tentative identification of the 7-HO-1P-AL-LAD impurity [Colour figure can be viewed at wileyonlinelibrary.com]

TABLE 1 ^1H and ^{13}C NMR data for 1P-AL-LAD hemitartrate in d_6 -DMSO at 600/150 MHz


No.	^{13}C [δ /ppm]	^1H [δ /ppm]
2	119.90	7.56 (d, $J = 1.9$ Hz, 1 H)
3	116.14	-
4	26.13	2.48–2.41 (m, H-4 α , 1 H) 3.52 (dd, $J = 15.2, 5.3$ Hz, H-4 β , 1 H)
5	58.82	3.35–3.32 (m, H-5 β , 1 H) * partially overlapping with H-21 (2 H)
6	-	-
7	51.51	3.07 (dd, $J = 11.3, 4.6$ Hz, H-7 α , 1 H) 2.58 (t, $J = 10.7$ Hz, H-7 β , 1 H)
8	39.08	3.77–3.71 (m, 8 α , 1 H)
9	122.31	6.34 (s, 1 H)
10	134.08	-
11	128.17	-
12	116.52	7.34–7.28 (m, 2 H) * partially overlapping with H-13
13	125.89	7.34–7.28 (m, 2 H) * partially overlapping with H-12
14	114.75	8.00 (d, $J = 7.6$ Hz, 1 H)
15	133.11	-
16	127.58	-
17	56.25	3.63 (dd, $J = 14.6, 4.9$ Hz, 1 H) 3.16 (dd, $J = 14.6, 8.0$ Hz, 1 H)
18	134.69	5.97 (dddd, $J = 17.1, 10.2, 7.9, 4.9$ Hz, 1 H)
19	118.03	5.30 (d, $J = 17.1$ Hz, 1 H); H-19 <i>trans</i> to H-18
19	118.03	5.20 (d, $J = 10.1$ Hz, 1 H); H-19 <i>cis</i> to H-18
20	170.52	-
21	41.56	3.42 (AB qq, $J = 13.9, 7.1$ Hz, 2 H).
21	39.72	3.32–3.27 (m, 2 H) *peaks are partially overlapping with H-5 β
22	14.82	1.20–1.14 (m, 6 H) *peaks are overlapping with H-25 (3 H)
22	13.07	1.05 (t, $J = 7.1$ Hz, 3 H)
23	172.49	-
24	28.17	3.00 (AB qq, $J = 14.0, 7.2$ Hz, 2 H)

TABLE 1 (Continued)



No.	¹³ C [δ/ppm]	¹ H [δ/ppm]
25	8.57	1.20–1.14 (m, 6 H) *peaks are overlapping with H-22 (3 H)
TA	173.16	–
TA	72.09	4.29 (s, ~1.3 H)

Abbreviation: TA, tartaric acid.

provisional identification of 7-HO-1P-AL-LAD was also consistent with m/z 86.0599 ($C_4H_8NO^+$) where the addition of the hydroxyl group led to a corresponding mass shift from m/z 70.0654 (1P-AL-LAD, $C_4H_8N^+$) (Figure 2b). Overall, this indicated that 7-HO-1P-AL-LAD might have been a synthesis by-product or formed during storage. The same impurity was also observed in the negative pHLM solution but it was not detected as a 1P-AL-LAD metabolite in the positive pHLM incubation mixture. As described below, its metabolite however was detected (7-HO-AL-LAD) following the hydrolysis of the propanoyl group.

The infrared spectrum recorded during the implementation of GC-sIR can be found as supporting information. Similar to other N^1 -propanoyl lysergamides (1P-LSD and 1P-ETH-LAD) investigated previously,^{20,26} indole NH bands were absent and two carbonyl stretches were detectable at 1704 and 1639 cm^{-1} . In 1P-LSD, these were recorded at 1703 and 1638 cm^{-1} whereas in 1P-ETH-LAD both carbonyl stretches were observed at 1704 and 1640 cm^{-1} . In the GC-sIR spectrum recorded from the N^1 -unsubstituted AL-LAD, the NH band was visible at around 3280 cm^{-1} together with only one carbonyl stretch at 1626 cm^{-1} .¹⁹ A spectrum obtained from the 1P-AL-LAD hemitartrate (2:1) salt using attenuated total reflectance Fourier transform infrared spectroscopy (ATR-FT-IR) has also been added in the supporting information.

Nuclear magnetic resonance (NMR) spectroscopy information is shown in Table 1 with full 1D/2D NMR spectra provided in the supporting information. Assignments were aided by 2D experiments (¹H/¹H correlation spectroscopy, COSY; ¹H/¹³C heteronuclear single quantum coherence spectroscopy, HSQC; ¹H/¹³C heteronuclear multiple bond correlation spectroscopy, HMBC) and essentially

comparable to the spectra recorded for AL-LAD during previous investigations¹⁹ with the main difference being the presence of the additional N^1 -propanoyl group in 1P-AL-LAD. For visual comparisons, AL-LAD proton and carbon NMR spectra together with 1P-AL-LAD spectra can be found in the supporting information as well. The estimated 1.12% iso-1P-AL-LAD impurity found in 1P-AL-LAD by LC-ESI-QTOF-MS was not observed in the proton NMR spectrum under the conditions used.

3.2 | Microsomal phase I metabolism of 1P-AL-LAD

In the pHLM assay, 14 phase I metabolites were detected and characterized. The metabolic reactions in vitro included hydroxylation of the core lysergamide ring or the N^6 -allyl group, formation of dihydrodiol metabolites, N -dealkylation, N^1 -deacylation, dehydrogenation, and combinations thereof. An overview of the QTOF-MS data of all detected and proposed in vitro metabolites of 1P-AL-LAD, their most abundant product ions and exact masses are presented in Table 2. Extracted ion chromatograms (EIC) using the protonated molecules are shown in Figure 4. An overview of the proposed metabolic pathways for 1P-AL-LAD is shown in Figure 5.

The main metabolite (peak height 5.10E+06 cps) could be unambiguously identified as AL-LAD (M12, $C_{22}H_{27}N_3O$, $[M + H]^+$, m/z 350.2223 Da), following hydrolysis of the N^1 -acyl substituent. The detection of AL-LAD in the pHLM-negative control sample (peak height 4.15E+05 cps) (supporting information) was hypothesized to

TABLE 2 1P-AL-LAD and its phase I metabolites along with their identification numbers (ID), retention times (RT), peak heights of the signal of the protonated molecule in MS1 (PH), accurate and exact mass to charge ratios, the respective error and the elemental compositions of the protonated molecule $[M + H]^+$ and its three most abundant fragment ions (FI A-C) with their relative ion intensities (rel. Ion. Int.)

ID	Compound	RT [min]	Ion	PH [cps]	Rel. Ion Int.	Accurate mass [m/z]	Elemental composition	Exact mass [m/z]	Error [ppm]	Rank
P	1P-AL-LAD	6.1	$[M + H]^+$	9.34E+05	-	406.2488	C ₂₅ H ₃₂ N ₃ O ₂	406.2489	-0.25	-
			FI A	-	100%	365.2097	C ₂₂ H ₂₇ N ₃ O ₂	365.2098	-0.27	
			FI B	-	51%	208.0994	C ₁₄ H ₁₂ N ₂	208.0995	-0.48	
			FI C	-	50%	264.1256	C ₁₇ H ₁₆ N ₂ O	264.1257	-0.38	
M1	1-Depropanoyl-di-hydrodiol-P1	3.1	$[M + H]^+$	1.43E+06	-	384.2282	C ₂₂ H ₃₀ N ₃ O ₃	384.2282	0.0	3
			FI A	-	100%	325.1783	C ₁₉ H ₂₃ N ₃ O ₂	325.1785	-0.62	
			FI B	-	53%	224.0939	C ₁₄ H ₁₂ N ₂ O	224.0944	-2.23	
			FI C	-	34%	223.0863	C ₁₄ H ₁₁ N ₂ O	223.0866	-1.34	
M2	1-Depropanoyl-N-deallyl-N-deethyl-P	3.2	$[M + H]^+$	9.54E+04	-	282.1601	C ₁₇ H ₂₀ N ₃ O	282.1601	0.0	13
			FI A	-	100%	209.1072	C ₁₄ H ₁₃ N ₂	209.1073	-0.48	
			FI B	-	25%	237.1016	C ₁₅ H ₁₃ N ₂ O	237.1022	-2.53	
			FI C	-	17%	183.0921	C ₁₂ H ₁₁ N ₂	183.0917	2.18	
M3	1-Depropanoyl-di-hydrodiol-P2	3.2	$[M + H]^+$	1.70E+05	-	384.2822	C ₂₂ H ₃₀ N ₃ O ₃	384.2822	0.0	10
			FI A	-	100%	224.0707	C ₁₄ H ₁₀ NO ₂	224.0706	0.47	
			FI B	-	83%	343.1891	C ₁₉ H ₂₅ N ₃ O ₃	343.1891	0.0	
			FI C	-	57%	315.1703	C ₁₈ H ₂₃ N ₂ O ₃	315.1703	0.0	
M4	1-Depropanoyl-hydroxy-P1	3.8	$[M + H]^+$	3.32E+05	-	366.2172	C ₂₂ H ₂₈ N ₃ O ₂	366.2176	-1.09	6
			FI A	-	100%	325.1783	C ₁₉ H ₂₃ N ₃ O ₂	325.1785	-0.62	
			FI B	-	44%	225.1017	C ₁₄ H ₁₃ N ₂ O	225.1022	-2.22	
			FI C	-	39%	224.0941	C ₁₄ H ₁₂ N ₂ O	224.0944	-1.34	
M5	1-Depropanoyl-N-deethyl-P	3.9	$[M + H]^+$	2.75E+06	-	322.1917	C ₂₉ H ₂₄ N ₃ O	322.1914	0.93	2
			FI A	-	100%	281.1523	C ₁₇ H ₁₉ N ₃ O	281.1523	0.0	
			FI B	-	81%	208.0995	C ₁₄ H ₁₂ N ₂	208.0995	0.0	
			FI C	-	24%	182.0840	C ₁₂ H ₁₀ N ₂	182.0838	1.10	
M6	1-Depropanoyl-hydroxy-P2	3.9	$[M + H]^+$	1.66E+05	-	366.2177	C ₂₂ H ₂₈ N ₃ O ₂	366.2176	0.27	11
			FI A	-	100%	325.1783	C ₁₉ H ₂₃ N ₃ O ₂	325.1785	-0.62	
			FI B	-	44%	225.1017	C ₁₄ H ₁₃ N ₂ O	225.1022	-2.22	
			FI C	-	39%	224.0941	C ₁₄ H ₁₂ N ₂ O	224.0944	-1.34	
M7	1-Depropanoyl-di-hydrodiol-P3	4.2	$[M + H]^+$	1.43E+05	-	384.2281	C ₂₂ H ₃₀ N ₃ O ₃	384.2282	-0.26	12
			FI A	-	71%	283.1441	C ₁₇ H ₁₉ N ₂ O ₂	283.1441	0.0	
			FI B	-	30%	208.0995	C ₁₄ H ₁₂ N ₂	208.0995	0.0	
			FI C	-	29%	309.1836	C ₁₉ H ₂₃ N ₃ O	309.1836	0.0	
M8	1-Depropanoyl-hydroxy-P3	4.2	$[M + H]^+$	1.79E+05	-	366.2176	C ₂₂ H ₂₈ N ₃ O ₂	366.2176	0	8
			FI A	-	100%	325.1783	C ₁₉ H ₂₃ N ₃ O ₂	325.1785	0.2	
			FI B	-	53%	224.0943	C ₁₄ H ₁₂ N ₂ O	224.0944	0.1	
			FI C	-	23%	207.0917	C ₁₄ H ₁₁ N ₂	207.0917	0	
M9	1-Depropanoyl-hydroxy-P4	4.3	$[M + H]^+$	1.74E+05	-	366.2176	C ₂₂ H ₂₈ N ₃ O ₂	366.2176	0	9
			FI A	-	100%	325.1780	C ₁₉ H ₂₃ N ₃ O ₂	325.1785	0.4	
			FI B	-	73%	224.0941	C ₁₄ H ₁₂ N ₂ O	224.0944	0.3	
			FI C	-	60%	207.0916	C ₁₄ H ₁₁ N ₂	207.0917	0.1	
M10	1-Depropanoyl-N-deallyl-P (Nor-LSD)	4.3	$[M + H]^+$	9.45E+05	-	310.1913	C ₁₉ H ₂₄ N ₃ O	310.1914	-0.32	4
			FI A	-	100%	209.1072	C ₁₄ H ₁₃ N ₂	209.1073	-0.48	
			FI B	-	67%	74.0966	C ₄ H ₁₂ N	74.0964	2.70	
			FI C	-	24%	237.1022	C ₁₅ H ₁₃ N ₂ O	237.1022	0.00	

TABLE 2 (Continued)

ID	Compound	RT [min]	Ion	PH [cps]	Rel. Ion Int.	Accurate mass [m/z]	Elemental composition	Exact mass [m/z]	Error [ppm]	Rank
M11	1-Depropanoyl-dehydro-P1	5.0	[M + H] ⁺	8.50E+04	100%	348.2069	C ₂₂ H ₂₆ N ₃ O	348.2070	-0.29	14
			FI A	-	21%	306.1600	C ₁₉ H ₂₀ N ₃ O	306.1601	-0.33	
			FI B	-	19%	235.0863	C ₁₅ H ₁₁ N ₂ O	235.0866	-1.28	
			FI C	-	6%	277.1337	C ₁₈ H ₁₇ N ₂ O	277.1335	0.72	
M12	AL-LAD (1-depropanoyl-P)	5.1	[M + H] ⁺	5.10E+06	-	350.2225	C ₂₂ H ₂₈ N ₃ O	350.2227	-0.57	1
			FI A	-	100%	208.0994	C ₁₄ H ₁₂ N ₂	208.0995	-0.48	
			FI B	-	81%	309.1835	C ₁₉ H ₂₃ N ₃ O	309.1836	-0.32	
			FI C	-	18%	207.0916	C ₁₄ H ₁₁ N ₂	207.0917	-0.48	
M13	N-Deallyl-P (1P-Nor-LSD)	5.3	[M + H] ⁺	1.91E+05	-	366.2177	C ₂₂ H ₂₈ N ₃ O ₂	366.2176	0.27	7
			FI A	-	100%	74.0966	C ₄ H ₁₂ N	74.0964	2.70	
			FI B	-	75%	265.1334	C ₁₇ H ₁₇ N ₂ O	265.1335	-0.38	
			FI C	-	46%	209.1073	C ₁₄ H ₁₃ N ₂	209.1073	0.00	
M14	1-Depropanoyl-dehydro-P2	5.5	[M + H] ⁺	5.13E+05	-	348.2071	C ₂₂ H ₂₆ N ₃ O	348.2070	0.29	5
			FI A	-	100%	208.0994	C ₁₄ H ₁₂ N ₂	208.0995	-0.48	
			FI B	-	51%	207.0918	C ₁₄ H ₁₁ N ₂	207.0917	0.48	
			FI C	-	43%	307.1678	C ₁₉ H ₂₁ N ₃ O	307.1679	-0.32	

Note: Metabolites were ranked from 1 (for most abundant) to 14 (for least abundant).

be a result of a spontaneous hydrolysis, which has also been reported previously for 1P-LSD.^{37,38} However, as described above, analysis of a 1P-AL-LAD solution also revealed the detection of about 0.64% of AL-LAD, which suggested that at least some proportion was present as an impurity. As shown in the supporting information, the detection of AL-LAD in the pHLM-positive incubation mixture confirmed its formation to a significant extent far beyond the very low abundance found in the pHLM-negative sample.

The second most abundant metabolite detected from the in vitro assay was the 1-depropanoyl-*N*-deethyl product (*N*-deethyl-AL-LAD, M5, C₂₀H₂₃N₃O, [M + H]⁺, *m/z* 322.19139 Da, peak height 2.75E+06 cps) following cleavage of both the 1-propanoyl group and one of the ethyl groups from the *N,N*-diethylamide moiety. Detection of the *N*¹-deacylated dihydrodiol metabolite M1 (C₂₂H₂₉N₃O₃, [M + H]⁺, *m/z* 384.2282 Da) showed a relatively high abundance (peak height 1.43E+06 cps). Although the exact position of the hydroxyl functions could not be assigned, the product ion spectrum of M1 suggested that the metabolic oxidations might have taken place on the phenyl part of the indole ring and on ring C (see supporting information for all ESI-QTOF-MS/MS data of metabolites). In comparison, metabolite M3 was another dihydrodiol isomer of M1 detected in a much lower abundance (peak height 1.70E+05 cps). By contrast, in M7 (C₂₂H₂₉N₃O₃, [M + H]⁺, *m/z* 384.2282 Da, peak height 1.43E+05 cps) the dihydrodiol group was located on the former *N*⁶-allyl side chain. Four mono hydroxylated metabolites (M4, M6, M8, M9, C₂₂H₂₇N₃O₂, [M + H]⁺, *m/z* 366.2176 Da) were formed after hydrolysis of the 1-propanoyl group. Oxidation/dehydration at the diethylamide moiety after *N*¹-deacylation led to the formation of metabolite M14 (C₂₂H₂₅N₃O, [M + H]⁺, *m/z* 348.2070 Da). The

metabolic cleavage of the *N*⁶-allyl group, which has also been described for AL-LAD previously,²⁵ was also represented by metabolites M2 (C₁₇H₁₉N₃O, [M + H]⁺, *m/z* 282.1601 Da), M10 (C₁₉H₂₃N₃O, [M + H]⁺, *m/z* 310.1913 Da), and M13 (C₂₂H₂₉N₃O₂, [M + H]⁺, *m/z* 366.2176 Da). However, estimation of abundance based on signal responses alone must be viewed with caution because the ionization efficiency for each metabolite might have been different and reference material would be needed in order to get more detailed insights.

As shown in Figure 4, a number of peaks were detected under EIC conditions in addition to the proposed metabolites. For example, in the M2 trace (*m/z* 282.1601), another peak labeled as 'artifact' was detected at 3.9 min that represented a fragment ion of M5 (¹³C isotope of *m/z* 281.1523). The EIC trace presenting *m/z* 366.2176 (M4, M6, M8, M9, M13) also contained a peak at 4.9 min and labeled as an impurity ("imp"). As described above (Figure 3), one minor impurity identified both in the negative pHLM mixture and 1P-AL-LAD solution was hypothesized to be 7-HO-1P-AL-LAD. Correspondingly, the positive pHLM incubation solution revealed the presence of the metabolic *N*¹-deacylation product of this impurity to form 7-HO-AL-LAD. The mass spectral data recorded for this metabolite is shown in Figure 6. The tentative identification process (including similarities with the tandem mass spectrum of AL-LAD; M12, supporting information), was similar to the one used above for 7-HO-1P-AL-LAD. The 'artifact' peak detected in the EIC trace of *m/z* 310.1914 (M10) at 5.1 min was identified as a fragment ion of M11 (¹³C isotope of *m/z* 309.1834). The peak eluting at 5.0 min in the trace presenting M11 (*m/z* 348.2070) might have reflected an isomer of M14 where another dehydro metabolite (double bond possibly between C4-C5,

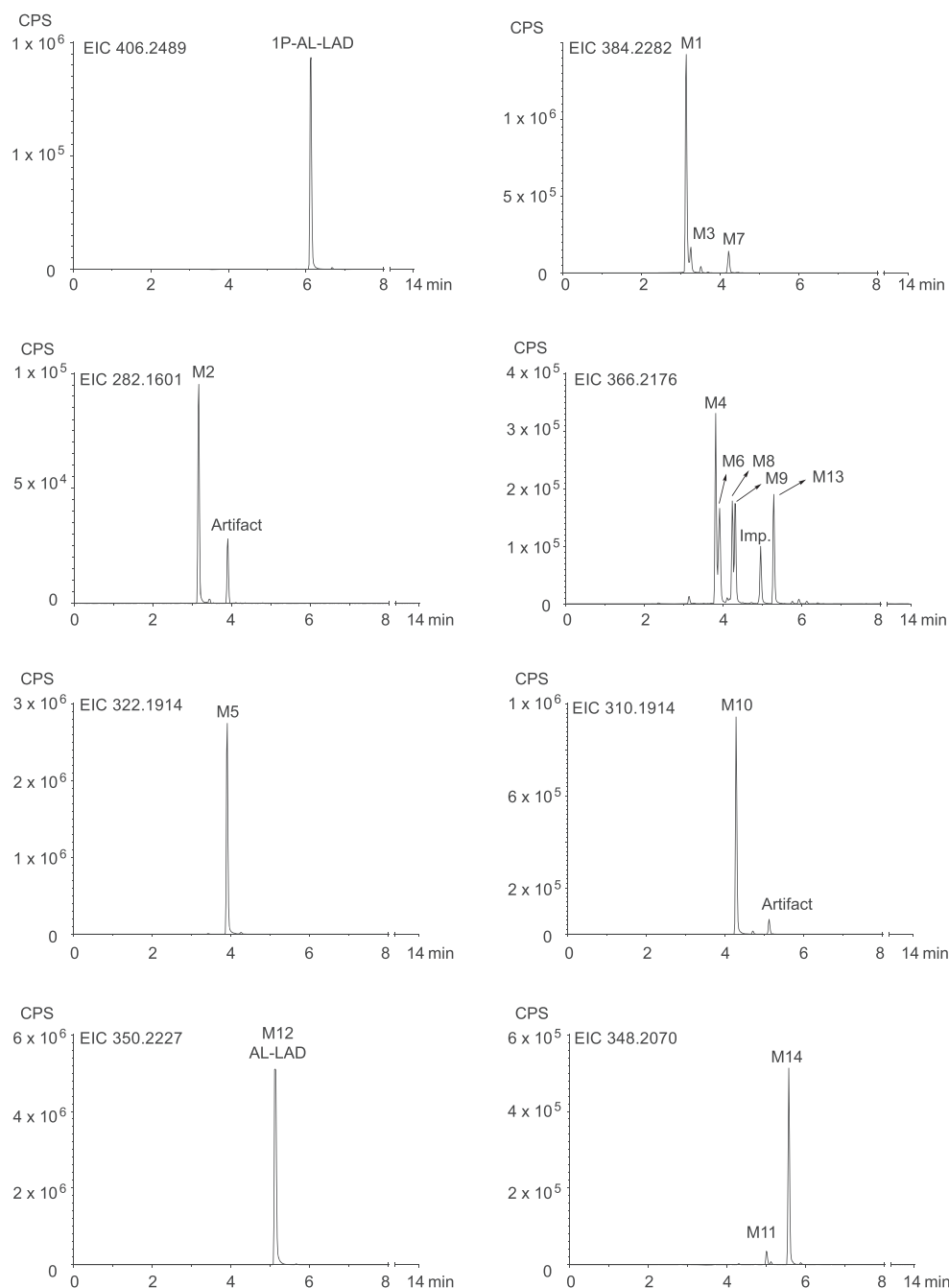


FIGURE 4 Extracted ion chromatograms using the protonated molecules of 1P-AL-LAD and its metabolites monitored by HPLC-ESI-QTOF-MS, numbering according to Table 2

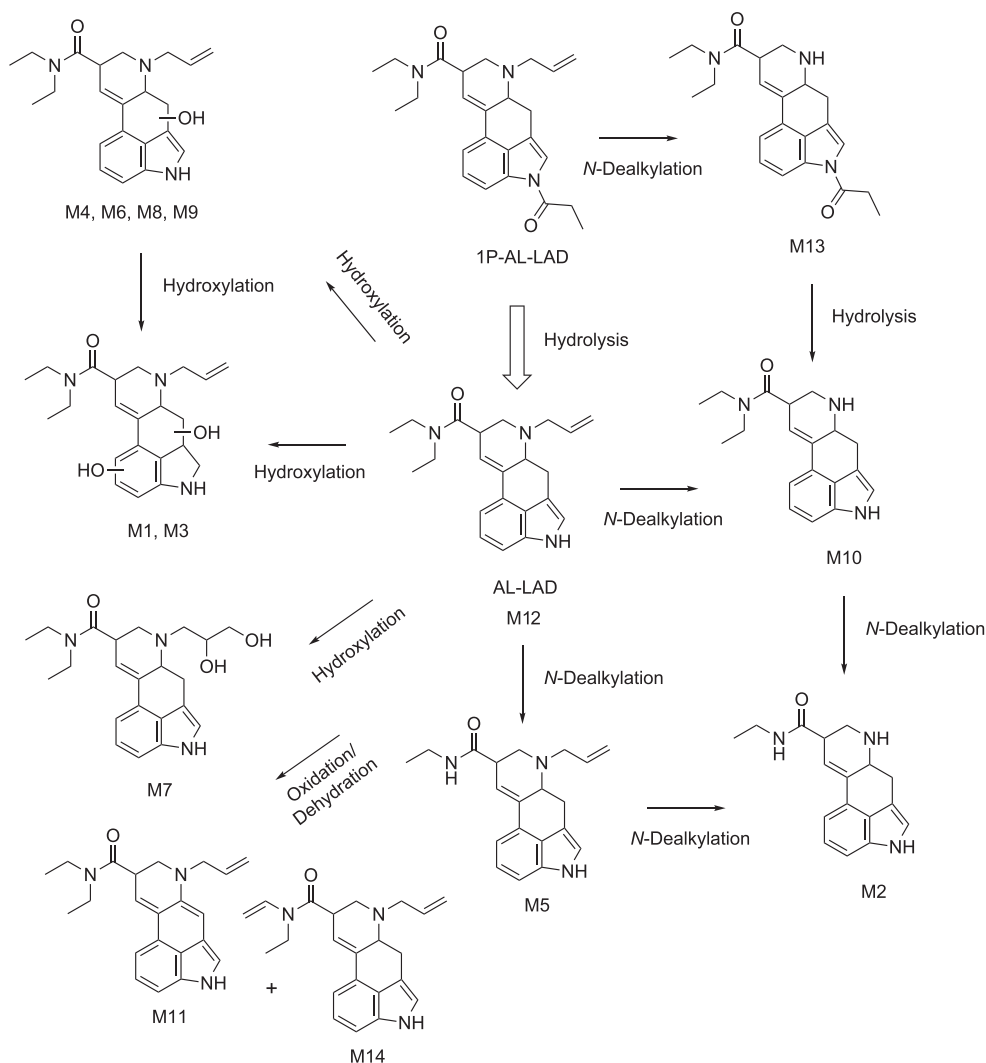
supporting information) might have been generated. The EIC of m/z 382.2125 ($C_{22}H_{28}N_3O_3$, $[M + H]^+$), showed four peaks in the pHLM positive incubations. The peak at 4.2 min could also be identified in the pHLM negative control and was interpreted as *N*-deethyl-hydroxy-1P-AL-LAD. Three further peaks eluting at 3.4, 3.6, and 3.8 min could indicate the enzymatically-catalyzed formation of 1-depropanoyl-di-hydroxy metabolites. However, the product ions detected for any of the signals (supporting information) seemed inconsistent with the data for di-hydroxy-AL-LAD, described by Wagmann et al.²⁵ Because mass spectral interpretation did not allow for a clear differentiation between dihydroxy and oxo-hydroxy

metabolites, and signal intensities were relatively low (peak height $<6.0E+04$ cps), these potential metabolites were not considered identifiable. However, they should be kept in mind, when biological samples are obtained, especially because the 2-oxo-3-hydroxy-LSD metabolite appeared to be a major metabolite of LSD.³⁹

3.3 | Head-twitch response

The 5-HT_{2A} receptor is the primary target for LSD and other psychedelic drugs in the brain.^{40,41} In mice, psychedelic drugs induce a

FIGURE 5 Postulated phase I metabolic pathways of 1P-AL-LAD studied by in vitro incubations with pooled human liver microsomes. Numbering according to Table 2



rapid side-to-side head shaking known as the head-twitch response (HTR). The HTR serves as a rodent behavioral proxy for human psychedelic effects and can be used to distinguish hallucinogenic and non-hallucinogenic 5-HT_{2A} agonists.⁴² HTR experiments were conducted with 1P-AL-LAD in male C57BL/6J mice to determine whether it has an LSD-like behavioral profile. After administration of 1P-AL-LAD to mice, there was a dose-dependent increase in HTR counts ($W(5,11.49) = 13.85$, $p = 0.0002$). The response induced by 1P-AL-LAD had an inverted U-shaped dose-response function (Figure 7), which is also the case for LSD and other psychedelic drugs.³⁵ The maximal response occurred after administration of 0.5 mg/kg 1P-AL-LAD ($p < 0.01$, Dunnett's T3 multiple comparisons test). The median effective dose (ED₅₀ value) for 1P-AL-LAD was 236 (95% CI: 155–322) µg/kg. Based on its molecular weight, 1P-AL-LAD induced the HTR with ED₅₀ = 491 (323–670) nmol/kg. The reported ED₅₀ for AL-LAD is 174.9 nmol/kg,¹⁹ making it about three times as potent as 1P-AL-LAD. In recent studies, 1P-LSD and 1cP-LSD were reported to induce the HTR with ED₅₀ values of 349.6 nmol/kg and 430 nmol/kg, making them slightly more potent than 1P-AL-LAD.^{26,29}

Previous studies have shown that N¹-acyl substitution reduces the affinity of LSD for the 5-HT_{2A} receptor and markedly dampens its agonist efficacy.³⁵ Nevertheless, N¹-acyl-substituted derivatives of LSD such as ALD-52 and 1P-LSD act as psychedelic drugs in humans and induce the HTR in mice, indicating those molecules retain the ability to activate the 5-HT_{2A} receptor after in vivo administration. Because there is evidence from both in vitro and in vivo studies that ALD-52 and 1P-LSD are metabolized to LSD,^{25,31,37} those molecules are believed to serve as prodrugs for LSD. Although AL-LAD has high affinity for the 5-HT_{2A} receptor ($K_i = 8.1$ nM for [³H]ketanserin-labeled sites in rat frontal cortex)⁴³ and acts as a 5-HT_{2A} agonist in calcium flux assays,⁴⁴ the activity of 1P-AL-LAD at the 5-HT_{2A} receptor is likely to be relatively weak because it contains an N¹-acyl group. Based on the pHLM data, 1P-AL-LAD is likely to be hydrolyzed to AL-LAD after administration to mice and therefore acts as a prodrug, similar to ALD-52 and 1P-LSD.

For LSD and a large series of psychedelic drugs, there is a robust correlation ($r = 0.9448$) between HTR ED₅₀ values in C57BL/6J mice and hallucinogenic potencies in humans.³⁵ When tested previously in HTR experiments, LSD (ED₅₀ = 132.8 nmol/kg)³⁴ and AL-LAD

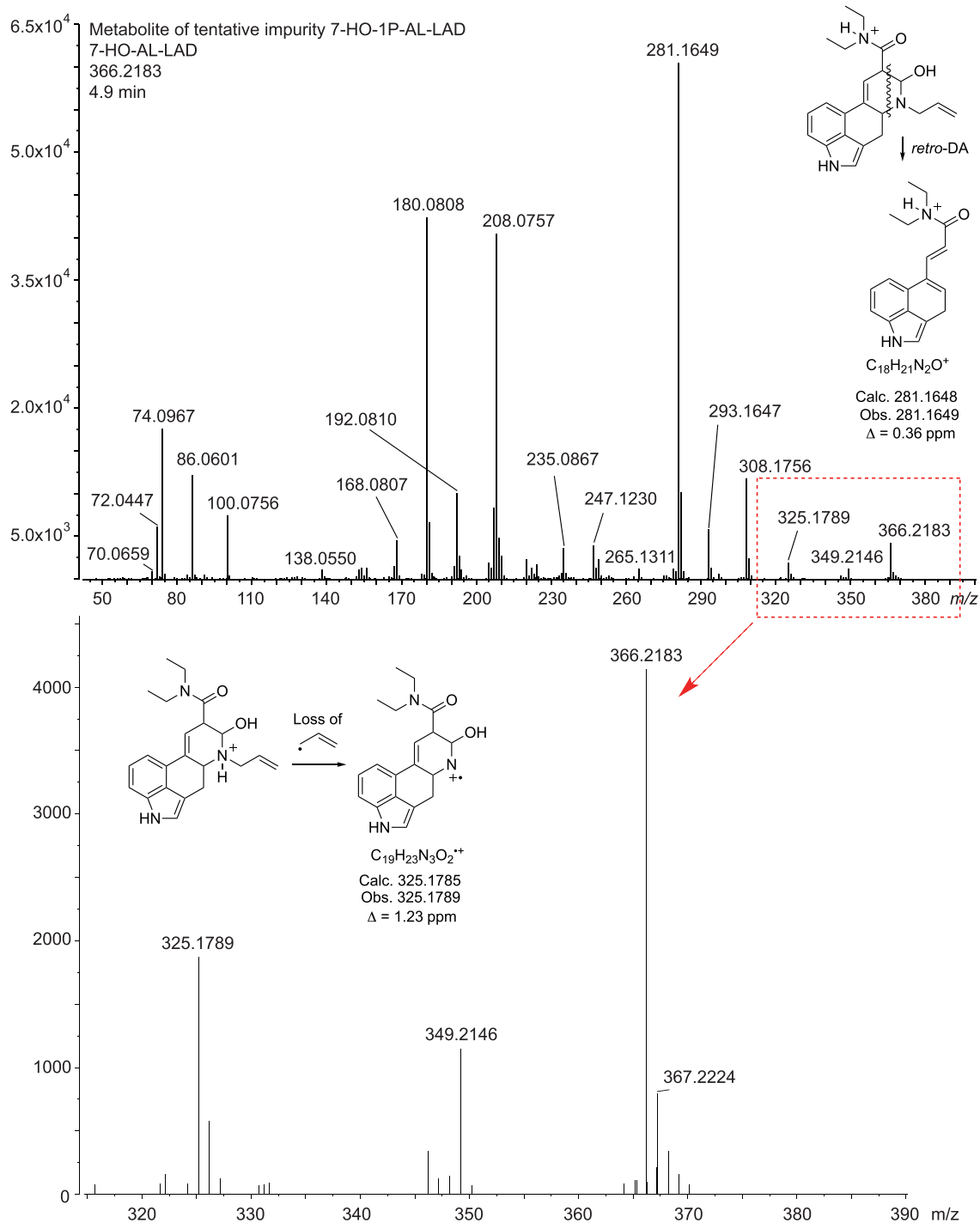


FIGURE 6 Tentative identification of 7-HO-AL-LAD labelled as “imp.” in the EIC trace at m/z 366.2176 (Figure 4) [Colour figure can be viewed at wileyonlinelibrary.com]

($ED_{50} = 174.9$ nmol/kg)¹⁹ had three to four times higher potency than 1P-AL-LAD. Although it is tempting to speculate based on the HTR data that 1P-AL-LAD may also have 3–4-fold lower potency than AL-LAD and LSD in humans, the relationship between psychedelic drug potencies in mice and humans may not extend to molecules acting as prodrugs. The identity and tissue expression of the

enzymes responsible for the hydrolysis of 1P-AL-LAD to AL-LAD may not be uniform across different species, potentially resulting in considerable cross-species variations in potency. Therefore, additional studies are warranted to understand the activity of 1P-AL-LAD in humans and to compare its potency relative to LSD and AL-LAD.

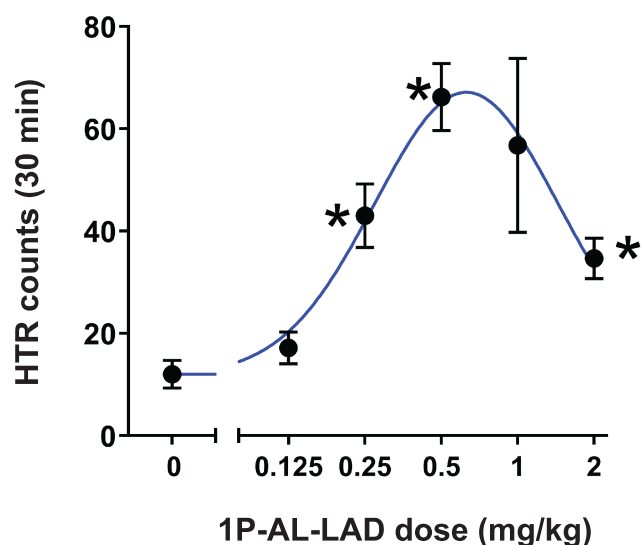


FIGURE 7 Dose-dependent increase of head-twitch response counts [Colour figure can be viewed at [wileyonlinelibrary.com](https://onlinelibrary.wiley.com)]

4 | CONCLUSION

Much of the interest in the properties of novel lysergamides reflects both the accumulating evidence of their therapeutic properties as well as their use and distribution as recreational drugs. 1P-AL-LAD is a relatively new addition to the lysergamide family. A comprehensive analytical characterization of 1P-AL-LAD was performed involving several forms of mass spectrometry, gas- and liquid chromatography, nuclear magnetic resonance spectroscopy and gas chromatography solid-phase infrared analysis aimed at supporting stakeholders interested in psychoactive drug research. Incubations with pooled human liver microsomes confirmed that 1P-AL-LAD is hydrolyzed to AL-LAD as the most abundant metabolite together with 13 other metabolites of varying signal response, which is consistent with the hypothesis that 1P-AL-LAD acts as a prodrug. The ability of 1P-AL-LAD to induce the HTR in mice shows it has a behavioral profile reminiscent of LSD and other serotonergic psychedelic drugs. Ultimately, human trials with 1P-AL-LAD are required to define its effects and abuse potential in humans.

ACKNOWLEDGEMENTS

The behavioral studies were supported by an award from the National Institute on Drug Abuse (NIDA) (R01 DA041336). The authors also thankfully acknowledge the support from the project ADEBAR *plus*, which is co-funded by the Internal Security Fund of the European Union (Grant IZ25-5793-2019-33). SDB thanks Sarah Gare for technical help and expresses gratitude to Stephen J. Chapman (Isomer Design, Toronto, Canada) for support. Open access funding enabled and organized by Projekt DEAL.

DATA AVAILABILITY STATEMENT

Data available in article supplementary material

ORCID

Simon D. Brandt <https://orcid.org/0000-0001-8632-5372>

Pierce V. Kavanagh <https://orcid.org/0000-0002-1613-3305>

Folker Westphal <https://orcid.org/0000-0003-0452-7814>

Benedikt Pulver <https://orcid.org/0000-0002-7772-2111>

Hannes M. Schwelm <https://orcid.org/0000-0001-7867-5831>

Kyla Whitelock <https://orcid.org/0000-0002-3675-2197>

Volker Auwärter <https://orcid.org/0000-0002-1883-2804>

Adam L. Halberstadt <https://orcid.org/0000-0001-5096-5829>

REFERENCES

- Dittrich A. The standardized psychometric assessment of altered states of consciousness (ASCs) in humans. *Pharmacopsychiatry*. 1998; 31(S 2):80-84. doi:[10.1055/s-2007-979351](https://doi.org/10.1055/s-2007-979351)
- Preller KH, Vollenweider FX. Phenomenology, structure, and dynamic of psychedelic states. *Curr Top Behav Neurosci*. 2018;18:221-256.
- Vollenweider FX, Smallridge JW. Classic psychedelic drugs: update on biological mechanisms. *Pharmacopsychiatry*. 2022. doi:[10.1055/a-1721-2914](https://doi.org/10.1055/a-1721-2914)
- Garcia-Romeu A, Richards WA. Current perspectives on psychedelic therapy: use of serotonergic hallucinogens in clinical interventions. *Int Rev Psychiatry*. 2018;30(4):291-316. doi:[10.1080/09540261.2018.1486289](https://doi.org/10.1080/09540261.2018.1486289)
- Mertens LJ, Preller KH. Classical psychedelics as therapeutics in psychiatry - current clinical evidence and potential therapeutic mechanisms in substance use and mood disorders. *Pharmacopsychiatry*. 2021;54(4):176-190. doi:[10.1055/a-1341-1907](https://doi.org/10.1055/a-1341-1907)
- Nichols DE, Walter H. The history of psychedelics in psychiatry. *Pharmacopsychiatry*. 2021;54(4):151-166. doi:[10.1055/a-1310-3990](https://doi.org/10.1055/a-1310-3990)
- Vollenweider FX, Preller KH. Psychedelic drugs: neurobiology and potential for treatment of psychiatric disorders. *Nat Rev Neurosci*. 2020;21(11):611-624. doi:[10.1038/s41583-020-0367-2](https://doi.org/10.1038/s41583-020-0367-2)
- Gasser P. Psychedelic group therapy. *Curr Top Behav Neurosci*. 2022. doi:[10.1007/7854_2021_1268](https://doi.org/10.1007/7854_2021_1268)
- Yockey RA, Vidourek RA, King KA. Trends in LSD use among US adults: 2015-2018. *Drug Alcohol Depend*. 2020;212:108071. doi:[10.1016/j.drugalcdep.2020.108071](https://doi.org/10.1016/j.drugalcdep.2020.108071)
- European Monitoring Centre for Drugs and Drug Addiction. European Drug Report 2021: Trends and Developments. Available at: <https://www.emcdda.europa.eu/system/files/publications/13838/TDAT21001ENN.pdf> [last accessed 15 February 2022].
- Pfaff RC, Huang X, Marona-Lewicka D, Oberlender R, Nichols DE. Lysergamides revisited. In: Lin GC, Glennon RA, eds. *Hallucinogens: An Update*. NIDA Research Monograph. Vol.146. Rockville, MD, USA: National Institute on Drug Abuse; 1994:52-73.
- Nichols DE. Chemistry and structure-activity relationships of psychedelics. *Curr Top Behav Neurosci*. 2018;36:1-43. doi:[10.1007/7854_2017_475](https://doi.org/10.1007/7854_2017_475)
- Niwaguchi T, Nakahara Y, Ishii H. Studies on lysergic acid diethylamide and related compounds. IV. Syntheses of various amide derivatives of norlysergic acid and related compounds. *Yakugaku Zasshi*. 1976;96(5):673-678. doi:[10.1248/yakushi1947.96.5_673](https://doi.org/10.1248/yakushi1947.96.5_673)
- Hashimoto H, Hayashi M, Nakahara Y, Niwaguchi T, Ishii H. Actions of D-lysergic acid diethylamide (LSD) and its derivatives on 5-hydroxytryptamine receptors in the isolated uterine smooth muscle of the rat. *Eur J Pharmacol*. 1977;45(4):341-348. doi:[10.1016/0014-2999\(77\)90273-4](https://doi.org/10.1016/0014-2999(77)90273-4)
- Hashimoto H, Hayashi M, Nakahara Y, Niwaguchi T, Ishii H. Hyperthermic effects of D-lysergic acid diethylamide (LSD) and its derivatives in rabbits and rats. *Arch Int Pharmacodyn Ther*. 1977;228(2): 314-321.

16. Hoffman AJ, Nichols DE. Synthesis and LSD-like discriminative stimulus properties in a series of *N*(6)-alkyl norlysergic acid *N,N*-diethylamide derivatives. *J Med Chem*. 1985;28(9):1252-1255. doi:10.1021/jm00147a022
17. Shulgin A, Shulgin A. *TIHKAL: The Continuation*. Berkeley, USA: Transform Press; 1997.
18. Shulgin AT. Basic pharmacology and effects. In: Laing R, Siegel JA, eds. *Hallucinogens. A Forensic Drug Handbook*. London: Academic Press; 2003:67-137.
19. Brandt SD, Kavanagh PV, Westphal F, et al. Return of the lysergamides. Part II: Analytical and behavioural characterization of *N*⁶-allyl-6-norlysergic acid diethylamide (AL-LAD) and (2'*S*,4'*S*)-lysergic acid 2,4-dimethylazetidide (LSZ). *Drug Test Anal*. 2017;9(1):38-50. doi:10.1002/dta.1985
20. Brandt SD, Kavanagh PV, Westphal F, et al. Return of the lysergamides. Part III: Analytical characterization of *N*⁶-ethyl-6-norlysergic acid diethylamide (ETH-LAD) and 1-propionyl ETH-LAD (1P-ETH-LAD). *Drug Test Anal*. 2017;9(10):1641-1649. doi:10.1002/dta.2196
21. European Monitoring Centre for Drugs and Drug Addiction (EMCDDA). EMCDDA-Europol 2015 Annual Report on the implementation of Council Decision 2005/387/JHA. EMCDDA, Lisbon, 2016. Available at: <http://www.emcdda.europa.eu/system/files/publications/2880/TDAS16001ENN.pdf> [Accessed 13 Feb 2022].
22. European Monitoring Centre for Drugs and Drug Addiction (EMCDDA). EMCDDA-Europol 2016 Annual Report on the implementation of Council Decision 2005/387/JHA. EMCDDA, Lisbon, 2017. Available at: http://www.emcdda.europa.eu/system/files/publications/4724/TDAN17001ENN_PDFWEB.pdf [accessed 13 Feb 2022].
23. Tanaka R, Kawamura M, Hakamatsuka T, Kikura-Hanajiri R. Identification and analysis of LSD derivatives in illegal products as paper sheet. *Yakugaku Zasshi J Pharm Soc Jpn*. 2020;140(5):739-750. doi:10.1248/yakushi.19-00230
24. Saeki Y, Sakamoto M, Shioda H, et al. Analytical results of new psychoactive substances-containing drugs purchased over the Internet in April 2019 - March 2020 and detection of new LSD analogs on blotter papers. *Ann Rep Tokyo Metr Inst Pub Health*. 2020;71:99-106.
25. Wagmann L, Richter LHJ, Kehl T, et al. In vitro metabolic fate of nine LSD-based new psychoactive substances and their analytical detectability in different urinary screening procedures. *Anal Bioanal Chem*. 2019;411(19):4751-4763. doi:10.1007/s00216-018-1558-9
26. Brandt SD, Kavanagh PV, Westphal F, et al. Return of the lysergamides. Part I: Analytical and behavioural characterization of 1-propionyl-*d*-lysergic acid diethylamide (1P-LSD). *Drug Test Anal*. 2016;8(9):891-902. doi:10.1002/dta.1884
27. Brandt SD, Kavanagh PV, Westphal F, et al. Return of the lysergamides. Part V: Analytical and behavioural characterization of 1-butanoyl-*d*-lysergic acid diethylamide (1B-LSD). *Drug Test Anal*. 2019;11(8):1122-1133. doi:10.1002/dta.2613
28. Brandt SD, Kavanagh PV, Westphal F, et al. Return of the lysergamides. Part VII: Analytical and behavioural characterization of 1-valeroyl-*D*-lysergic acid diethylamide (1V-LSD). *Drug Test Anal*. 2021;14(4):733-740. doi:10.1002/dta.3205
29. Brandt SD, Kavanagh PV, Westphal F, et al. Return of the lysergamides. Part VI: Analytical and behavioural characterization of 1-cyclopropanoyl-*d*-lysergic acid diethylamide (1CP-LSD). *Drug Test Anal*. 2020;12(6):812-826. doi:10.1002/dta.2789
30. Johnson MP, Loncharich RJ, Baez M, Nelson DL. Species variations in transmembrane region V of the 5-hydroxytryptamine type 2A receptor alter the structure-activity relationship of certain ergolines and tryptamines. *Mol Pharmacol*. 1994;45(2):277-286.
31. Halberstadt AL, Chatha M, Klein AK, et al. Pharmacological and bio-transformation studies of 1-acyl-substituted derivatives of *d*-lysergic acid diethylamide (LSD). *Neuropharmacology*. 2020;172:107856. doi:10.1016/j.neuropharm.2019.107856
32. European Monitoring Centre for Drugs and Drug Addiction (EMCDDA). EMCDDA-Europol 2017 Annual Report on the implementation of Council Decision 2005/387/JHA. EMCDDA, Lisbon, 2018. Available at: https://www.emcdda.europa.eu/system/files/publications/9282/20183924_TDAN18001ENN_PDF.pdf
33. Halberstadt AL, Geyer MA. Effect of hallucinogens on unconditioned behavior. *Curr Top Behav Neurosci*. 2018;36:159-199. doi:10.1007/7854_2016_466
34. Halberstadt AL, Geyer MA. Characterization of the head-twitch response induced by hallucinogens in mice: detection of the behavior based on the dynamics of head movement. *Psychopharmacology (Berl)*. 2013;227(4):727-739. doi:10.1007/s00213-013-3006-z
35. Halberstadt AL, Chatha M, Klein AK, Wallach J, Brandt SD. Correlation between the potency of hallucinogens in the mouse head-twitch response assay and their behavioral and subjective effects in other species. *Neuropharmacology*. 2020;167:107933. doi:10.1016/j.neuropharm.2019.107933
36. Halberstadt AL. Automated detection of the head-twitch response using wavelet scalograms and a deep convolutional neural network. *Sci Rep*. 2020;10(1):8344. doi:10.1038/s41598-020-65264-x
37. Grumann C, Henkel K, Brandt SD, Stratford A, Passie T, Auwärter V. Pharmacokinetics and subjective effects of 1P-LSD in humans after oral and intravenous administration. *Drug Test Anal*. 2020;12(8):1144-1153. doi:10.1002/dta.2821
38. Grumann C, Henkel K, Stratford A, et al. Validation of an LC-MS/MS method for the quantitative analysis of 1P-LSD and its tentative metabolite LSD in fortified urine and serum samples including stability tests for 1P-LSD under different storage conditions. *J Pharm Biomed Anal*. 2019;174:270-276. doi:10.1016/j.jpba.2019.05.062
39. Libânio Osório Marta RF. Metabolism of lysergic acid diethylamide (LSD): an update. *Drug Metab Rev*. 2019;51(3):378-387. doi:10.1080/03602532.2019.1638931
40. Halberstadt AL. Recent advances in the neuropsychopharmacology of serotonergic hallucinogens. *Behav Brain Res*. 2015;277:99-120. doi:10.1016/j.bbr.2014.07.016
41. Nichols DE. Psychedelics. *Pharmacol Rev*. 2016;68(2):264-355. doi:10.1124/pr.115.011478
42. González-Maeso J, Weisstaub NV, Zhou M, et al. Hallucinogens recruit specific cortical 5-HT_{2A} receptor-mediated signaling pathways to affect behavior. *Neuron*. 2007;53(3):439-452. doi:10.1016/j.neuron.2007.01.008
43. Watts VJ, Lawler CP, Fox DR, Neve KA, Nichols DE, Mailman RB. LSD and structural analogs: pharmacological evaluation at D₁ dopamine receptors. *Psychopharmacology (Berl)*. 1995;118(4):401-419. doi:10.1007/BF02245940
44. McCorvy JD. *Mapping the binding site of the 5-HT_{2A} receptor using mutagenesis and ligand libraries: Insights into the molecular actions of psychedelics*. Ph. D. Thesis, Purdue University, West Lafayette, Indiana, USA. 2012.

SUPPORTING INFORMATION

Additional supporting information may be found in the online version of the article at the publisher's website.

How to cite this article: Brandt SD, Kavanagh PV, Westphal F, et al. Analytical profile, in vitro metabolism and behavioral properties of the lysergamide 1P-AL-LAD. *Drug Test Anal*. 2022;14(8):1503-1518. doi:10.1002/dta.3281